Cement & Concrete Composites 34 (2012) 172–184

Contents lists available at SciVerse ScienceDirect

Cement & Concrete Composites

journal homepage: www.elsevier.com/locate/cemconcomp

Tensile behavior of Ultra High Performance Hybrid Fiber Reinforced Concrete

Seung Hun Park [a], Dong Joo Kim [a,*], Gum Sung Ryu [b], Kyung Taek Koh [b]

[a] Department of Civil and Environmental Engineering, Sejong University, 98 Gunja-Dong, Gwangjin-Gu, Seoul 143-747, Republic of Korea
[b] Korea Institute of Construction Technology, 2311 Daewha-Dong, Ilsan-Gu, Goyang-Si, Gyeonggi-Do 411-712, Republic of Korea

ARTICLE INFO

Article history:
Received 11 January 2011
Received in revised form 7 September 2011
Accepted 8 September 2011
Available online 13 September 2011

Keywords:
Blending effect
Hybrid fiber composite
Macro-fiber
Micro-fiber
Ultra High Performance Fiber Reinforced Concrete

ABSTRACT

The effects of blending fibers on the tensile behavior of Ultra High Performance Hybrid Fiber Reinforced Concrete (UHP-HFRC) are investigated. Four types of steel macro-fibers (of differing length or geometry) and one type of steel micro-fiber are considered. In producing the specimens, the volume content of the macro-fiber was held at 1.0%, whereas the volume content of the micro-fiber varied from 0.0% to 1.5%. The overall shape of tensile stress–strain curves of UHP-HFRC is primarily dependent upon the type of macro-fiber, although the addition of micro-fibers favorably affects the strain hardening and multiple cracking behaviors. UHP-HFRC produced from macro-fibers with twisted geometry provides the best performance with respect to post cracking strength, strain capacity and multiple micro-cracking behavior, whereas UHP-HFRC produced with long, smooth macro-fibers exhibits the worst performance.

1. Introduction

Although the brittle behavior of Ultra High Performance Concrete (UHPC) has been one of main obstacles for its practical application, UHPC has demonstrated superior mechanical and material properties, e.g., ultra high compressive strength (150–200 MPa) and dense matrix structure [6–8,23]. As a result, various approaches have been investigated to remedy its brittle failure [1,2,4,5,14,20,24]. However, the achievement of strain hardening behavior with strain capacities of more than 0.2% has been a challenge, particularly with UHPC matrices reinforced with short, smooth steel fibers. A large amount ($V_f = 4 \sim 6\%$) of short, smooth steel fibers has been generally required to produce strain hardening behavior in UHPC matrices due to the relatively low bond strength of such fibers. The large amounts of fiber significantly increases the cost of UHPFRC since only 1% fiber volume content can be more expensive than the matrix material. Thus, from a cost perspective, the fiber volume contents should be minimized for practical application of UHPFRC.

Wille et al. [24] recently produced strain hardening behavior, with 14.2 MPa post-cracking strength and 0.24% strain capacity, by using only 2.5% short, smooth steel fibers ($d_f = 0.2$ mm, $L = 13$ mm) in an UHPC matrix. They reported good tensile performance of UHPFRCs with 2% high strength deformed steel fibers, such as hooked and twisted steel fibers. Their investigation focused on the tensile response of Ultra High Performance-Mono Fiber Reinforced Concrete (UHP-MFRC).

Nonetheless, using a type of fiber in UHPC, it is still difficult to obtain strain capacity more than 0.5%, as well as tensile post-cracking strength more than 15 MPa, for the two following reasons. First, there is a limit in the amount of fiber volume contents that can be mixed, especially for deformed steel macro-fibers with an aspect ratio more than 80 and length longer than 30 mm. Second, the bond strength of short micro-fiber is much weaker than that of deformed steel macro-fiber, although a much larger amount (4.0–6.0%) of fibers can be added without serious reduction in workability. Thus, it has been hard to obtain strain hardening behavior with strain capacity more than 0.25% by using micro-fibers only.

The approach selected in this research is to blend macro- and micro-fibers in a UHPC matrix to enhance both the post cracking strength (tensile strength) and strain capacity (ductility) of UHPFRCs by using a small amount of fibers without reduction in workability. In blending macro- and micro-fibers, it is expected that macro-fibers are more effective in increasing ductility while micro-fibers are effective in enhancing tensile strength. However, there is still little information on the tensile stress–strain response of such Ultra High Performance-Hybrid Fiber Reinforced Concretes (UHP-HFRC). In addition, current UHP-HFRCs require great amounts of fiber contents, 4–11% by volume, as summarized in Table 1, and consequently, they tend to be too expensive. This situation has motivated the experimental study, reported in this paper, which focuses on the tensile response of UHP-HFRC with low fiber contents (a maximum of 2.5% by volume). This is accomplished by

* Corresponding author. Tel.: +82 2 3408 3820; fax: +82 2 3408 4332.
E-mail addresses: parksh8179@naver.com (S.H. Park), djkim75@sejong.ac.kr (D.J. Kim), ryu0505@kict.re.kr (G.S. Ryu), ktgo@kict.re.kr (K.T. Koh).

0958-9465/$ - see front matter © 2011 Elsevier Ltd. All rights reserved.
doi:10.1016/j.cemconcomp.2011.09.009

Table 1
Tensile properties of UHPFRCs.

Name	Type (# of fiber types)	Total fiber volume contents %	Fiber 1			Fiber 2			Mechanical properties			Reference
			l_f (mm)	d_f (mm)	V_f (%)	l_f (mm)	d_f (mm)	V_f (%)	σ_{pc} (MPa)	ε_{pc} (%)	$f'c$ (MPa)	
DUCTAL	Mono (1)	2.0	13–15	0.2	Smooth 2.0	–	–	–	12.0	0.3	160–240	Chanvillard and Rigaud [4]
CERACEM	Mono (1)	2.5	20	0.3	Smooth 2.5	–	–	–	9.9	0.025	199	Jungwirth and Muttoni [9] Maeder et al. [14]
UHPFRC1	Mono (1)	6.0	10	0.2	Smooth 6.0	–	–	–	9.65	0.07	150–200	Wuest et al. [25]
UHPFRC2	Mono (1)	4.0	13	0.16	Smooth 4.0				12.6	0.27	150–200	Wuest et al. [25]
S-UHPFRC	Mono (1)	2.5	13	0.2	Smooth 2.5				14.2	0.24	200	[23,24]
T-UHPFRC	Mono (1)	2.0	30	0.3	Twisted 2.0	–	–	–	14.9	0.61	200	[23,24]
H-UHPFRC	Mono (1)	2.0	30	0.375	Hooked 2.0				14.0	0.45	200	[23,24]
HFC	Hybrid (2)	1.5	60	0.7	Hooked 1.0	13	0.2	Smooth 0.5%	12	–	120.1	Markovic [15]
HFC	Hybrid (2)	1.5	60	0.7	Hooked 0.5	13	0.2	Smooth 1.0%	9–10	–	125.0	Markovic [15]
CARDIFRC	Hybrid (2)	6.0	13	0.16	Smooth 5.0	6	0.16	Smooth 1.0%	13.5	0.06	200	Farhat et al. [5], Benson and Karihaloo [2]
MSCC	Hybrid (2)	7.0	25	0.3	Hooked 2.0	5	0.25	Smooth 5.0%	15.0	–	193.3	Rossi [21]
CEMTEC*	Hybrid (3)	11.0							20.0	0.2	200	Boulay et al. [3] Rossi et al. [20]

* Detailed information about the types of fiber used in CEMTEC are not provided in Boulay et al. [3] Rossi et al. [20].

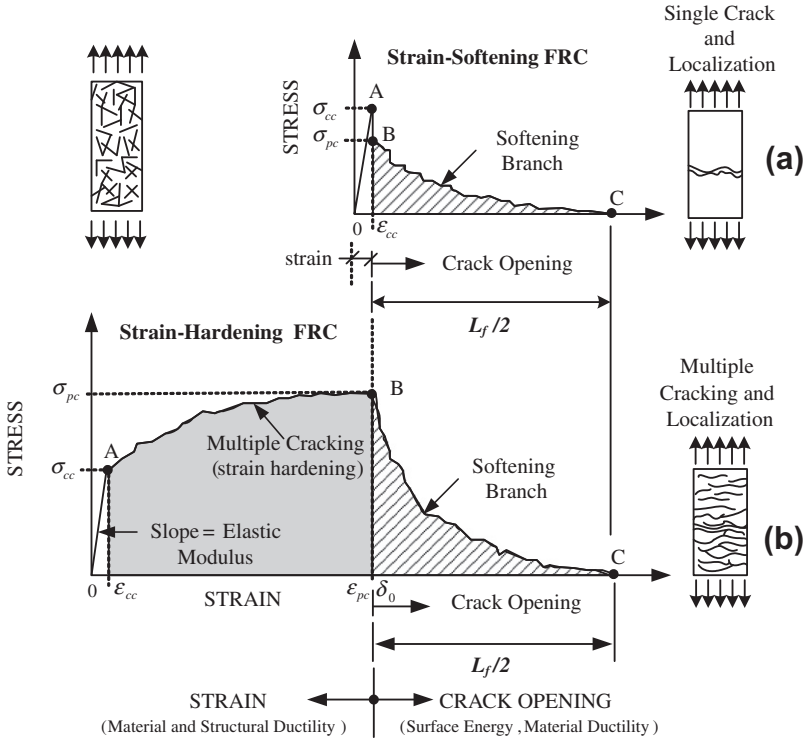

Fig. 1. Typical tensile strain softening and hardening behavior of FRC, HPFRCC and UHPFRC.

Table 2
Composition of matrix mixtures by weight ratio and compressive strength [19, 22].

Cement (Type I)	Silica fume	Silica sand	Glass (silica) powder	Super-plasticizer	Water	f'_c, ksi (MPa)
1.00	0.25	1.10	0.30	0.067	0.20	29.0 (200)

Table 3
Properties of fibers.

Fiber type	Name (notation)	Diameter in (mm)	Length in (mm)	Length/diameter	Density g/cc	Tensile strength ksi (MPa)	Elastic modulus ksi (GPa)
Macro	Smooth (SL-)	0.012 (0.3)	1.181 (30)	100	7.9	373.9 (2580)	29,000 (200)
	Hooked A (HA-)	0.015 (0.375)	1.181 (30)	80	7.9	334.9 (2311)	29,000 (200)
	Hooked B (HB-)	0.031 (0.775)	2.441 (62)	80	7.9	274.1 (1891)	29,000 (200)
	Twisted (T-)	0.015 (0.3)*	1.181 (30)	100	7.9	351.8 (2428)**	29,000 (200)
Micro	Smooth (SS-)	0.008 (0.2)	0.512 (13)	65	7.9	404.0 (2788)	29,000 (200)

* Equivalent diameter.
** Tensile strength of the fiber after twisting.

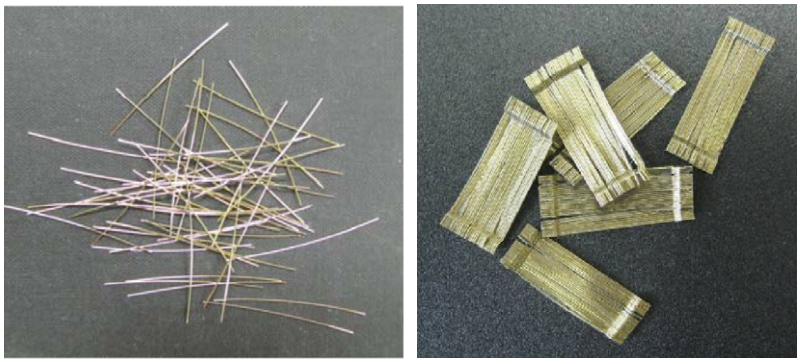

(a) Long smooth macro fiber (b) Hooked A macro fiber

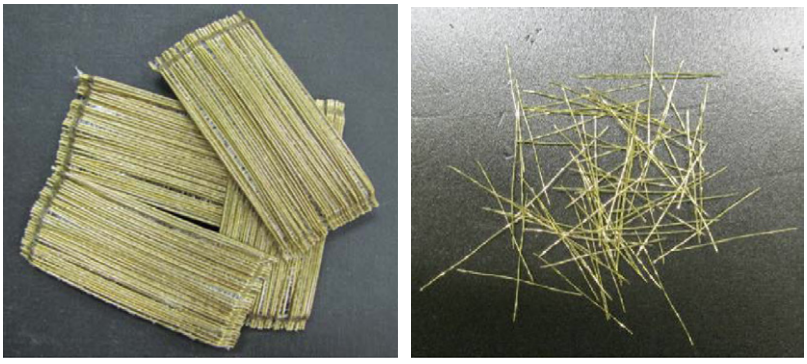

(c) Hooked B macro fiber (d) Twisted macro fiber

(e) Short smooth micro fiber

Fig. 2. Images of fibers: (a) Long smooth macro-fiber; (b) hooked A macro-fiber; (c) hooked B macro-fiber; (d) twisted macro-fiber; and (e) short smooth micro fiber.

blending one of four different types of steel macro-fiber (which differ in length or geometry) with steel micro-fibers.

The aim of this research is to investigate the effects of blending macro- and micro-fibers on the tensile behavior of UHP-HFRCs. The specific objectives are to investigate (1) the influence of adding micro-fibers on the strain hardening and multiple cracking behavior of UHP-HFRCs, and (2) how the different types of macro-fiber influence performance outcomes of the hybrid fiber systems.

2. Ultra High Performance Fiber Reinforced Concrete

Current UHPFRCs are classified into three groups according to the type of fiber used in UHPC matrices. In the first group, high strength smooth steel fibers with very fine diameter ($d_f \leqslant 0.2$ mm) and relatively short fiber length ($L_f \leqslant 13$ mm) have been commonly applied in UHPC matrices [4,25]. In this group, a large amount of short smooth steel fibers ($V_f = 4$–6%) has been generally required to obtain the strain hardening behavior as summarized in Table 1. Moreover, the strain capacity ($\varepsilon_{pc} \leqslant 0.25\%$) of UHPFRC in first group is much lower than that ($\varepsilon_{pc} \approx 0.5\%$) of UHPFRC using high strength deformed steel fibers in second group as shown in Table 1.

Table 4
Test matrix.

Type of macro-fiber (V_f = 1.0%)	Micro fiber volume content (%)	Notation
Long smooth (LS-)	0.0	LS10SS00
	0.5	LS10SS05
	1.0	LS10SS10
	1.5	LS10SS15
Hooked A (HA-)	0.0	HA10SS00
	0.5	HA10SS05
	1.0	HA10SS10
	1.5	HA10SS15
Hooked B (HB-)	0.0	HB10SS00
	0.5	HB10SS05
	1.0	HB10SS10
	1.5	HB10SS15
Twisted (T-)	0.0	T10SS00
	0.5	T10SS05
	1.0	T10SS10
	1.5	T10SS15

In the second group, relatively a small amount ($V_f \leqslant 2.0\%$) of high strength deformed steel fibers, e.g., high strength hooked (H-) and twisted (T-) fibers, was reinforced in a UHPC matrix to produce the strain hardening behavior accompanied with multiple micro-cracks [24]. The high strength deformed steel fibers in the second group are longer ($L_f \geqslant 30$ mm) and thicker ($d_f \geqslant 0.3$ mm) than the short smooth steel fibers used in the first group. The deformed steel fibers show slip-hardening behavior [11], while the smooth steel fibers produce slip-softening behavior in a mortar matrix with 84 MPa compressive strength. Although both deformed steel fibers shows slip-hardening behavior, the T-fiber generates two to five times higher equivalent bond strength compared to that of the H-fiber. The higher equivalent bond strength is favorable for strain hardening with multiple micro-cracks [10–12]. Recently, Wille et al. [24] reported that UHPFRC using only 2% T-fibers produced a high post-cracking strength (≈15 MPa) and a high strain capacity (≈0.5%), as summarized in Table 1. However, there is a limit in the amount of deformed steel fibers that can be mixed since the higher aspect ratio and longer length of deformed steel fibers causes a serious reduction in workability. Based on authors' experience regarding T-fibers having 30 mm length and 0.3 mm diameter, it is very difficult to produce mixtures with more than 2.0% fiber volume content.

In third group are UHP-HFRCs, which blend two or three different types of fibers in UHPC matrices [21,20,3,5,2]. These materials blend long and short fibers, or smooth and hooked steel fibers. The

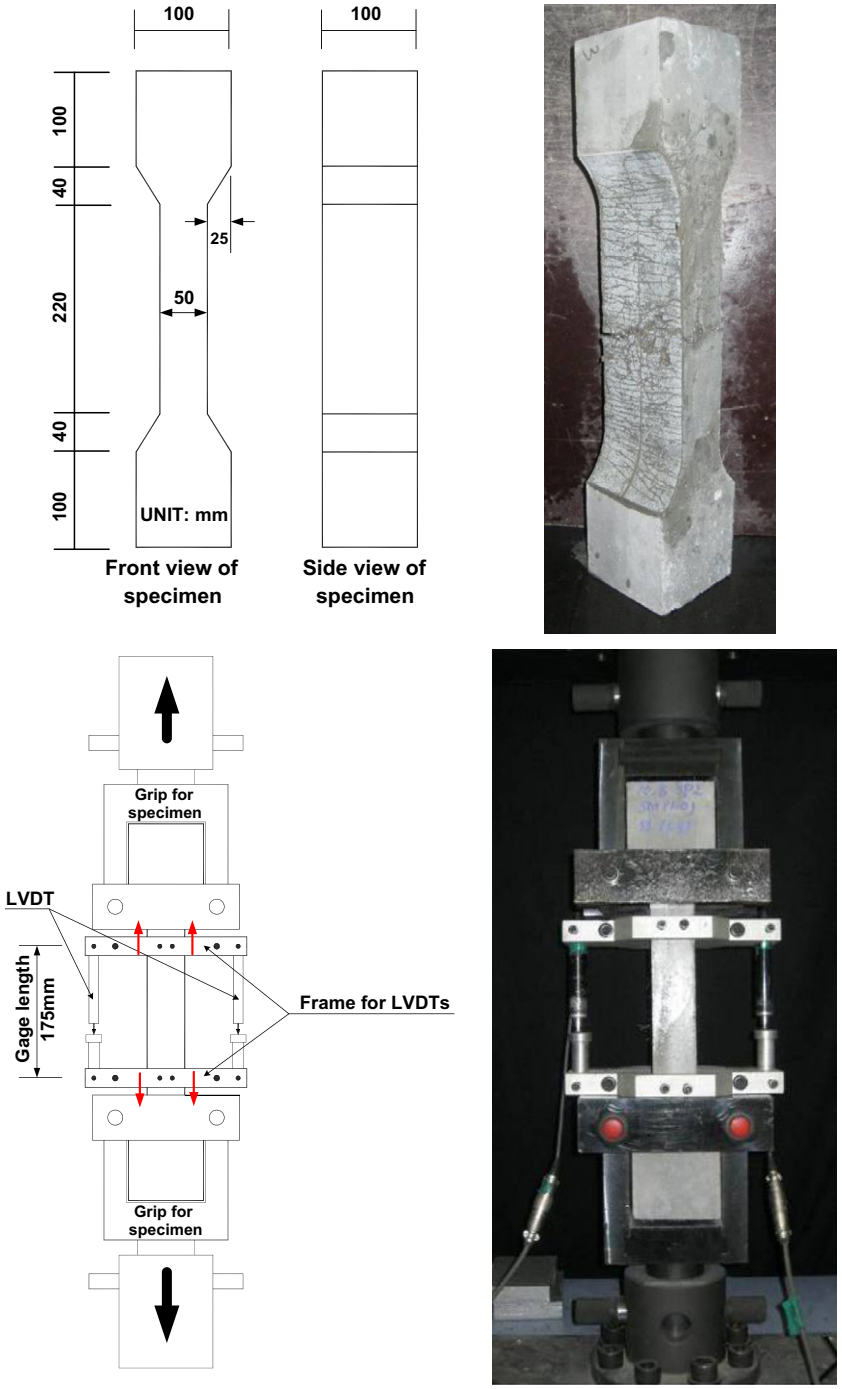

Fig. 3. Tensile specimen geometry and test set-up.

volume fractions of fibers used, as shown in Table 1, are between 6% and 11% [21,20,3,5,2]. The large amount of fibers is still one of main difficulties in the application of UHP-HFRCs due to their high material cost. In addition, the reported mechanical properties of UHP-HFRC are mostly with respect to the flexural behavior under four point bending. Markovic [15] reported the flexural and tensile behavior of hybrid FRC with a compressive strength of 120–140 MPa; however, no information about tensile strain capacity and multiple micro-cracking behavior was provided, because the section width was not constant along the height of the tensile specimens. Consequently, very little information is available regarding the tensile stress–strain response of UHP-HFRCs. Rossi [20,21] described the development of Multi-scale Cement Composites (MSCC) and CEMTEC$_{multiscale}$ by blending two to three types of steel fibers in the UHPC matrix with 7–11% fiber content by volume. Although both MSCC and CEMTEC$_{multiscale}$ produced very high tensile strength (more than 15 MPa), their strain capacity was lower than 0.3%. Benson and Karihaloo [2] also examined the development of hybrid steel fiber reinforced UHPFRC named CARDIFRC using 6% fiber volume content. They obtained a 13.5 MPa post-cracking tensile strength and a 0.06% strain capacity.

3. Strain hardening condition and tensile parameters

To obtain the strain hardening behavior as shown in Fig. 1, the post cracking strength (σ_{pc}) at point B should be higher than the first cracking strength (σ_{cc}) at point A, as expressed by Eq. (1). The first cracking strength (σ_{cc}) is mainly influenced by the tensile strength of the matrix, whereas the post cracking strength (σ_{pc}) is determined by the fiber bridging capacity, which is a function of fiber factor ($V_f \cdot L_f/d_f$) and bond strength (τ) [18,17].

$$\text{Strain hardening condition} : \sigma_{pc}/\sigma_{cc} \geqslant 1 \quad (1)$$

The strain value at post cracking strength σ_{pc} is defined as strain capacity ε_{pc} of UHPFRC. The number of multiple micro-cracks within gage length of specimens is also estimated, and the average crack spacing is calculated by dividing the gage length with the number of cracks.

The effect of blending macro- and micro-fibers on the tensile parameters of UHP-HFRCs is investigated by conducting the following experimental program. The quantities of interest include σ_{cc}, ε_{pc}, σ_{pc}, and the number of micro-cracks.

4. Experimental program

The experimental program is designed to understand: (1) whether the addition of micro-fibers in the hybrid system favors strain hardening and multiple cracking behavior (i.e., as the amount of micro-fiber increases, is the enhancement of σ_{pc} higher than that of σ_{cc} ?); and (2) whether the addition of micro-fibers, regardless of the type of macro-fiber in the hybrid system, produces identical enhancement of tensile properties.

4.1. Materials

The compressive strength of the UHPC matrix used for all specimens is 29 ksi (200 MPa), and the matrix composition was given by Park et al. [19]. The silica sand used in the matrix has a diameter

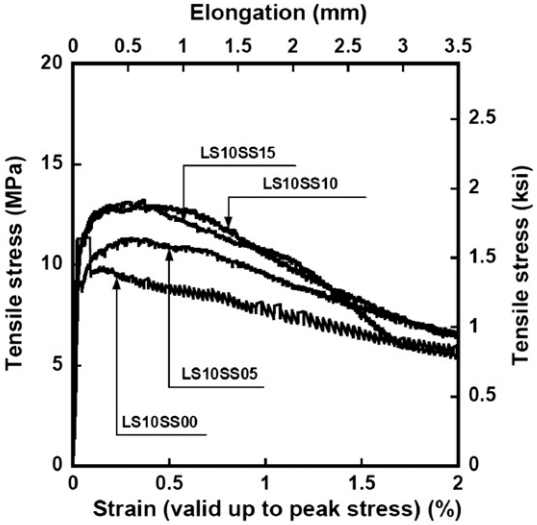

(a) Average tensile stress – strain curves

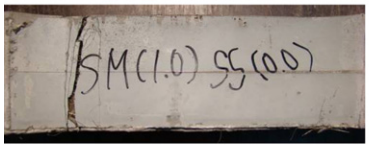

(b) Cracking behavior of LS10SS00

(c) Cracking behavior of LS10SS05

(d) Cracking behavior of LS10SS10

(e) Cracking behavior of LS10SS15

Fig. 4. Tensile test results with high strength long smooth fiber (LS-fiber) as the macro-fiber.

lower than 0.5 mm. Glass powder, used as a filler in the matrix, has 10 μm average diameter. The composition of the glass powder is 98% SiO_2, and its density is 2.60 g/cm^3(0.0939*lb*/in.^{3}). The four macro-fibers studied are long smooth steel fiber (LS-), two types of hooked fiber (HA- and HB-), and twisted (T-) steel fibers. The volume content of the macro-fibers is maintained as 1.0% for workability, while the volume contents of the micro-fibers blended, shorter smooth steel fibers (SS-), varied at 0.0%, 0.5%, 1.0% and 1.5%. Table 2 provides the matrix composition of the UHPC matrix used and its average compressive strength. Fiber properties are given in Table 3 and Fig. 2 show images of each fiber type. The T-fibers investigated have triangular section and six ribs in 30 mm fiber length. The consideration of the four types of macro-fiber and four volume contents of micro-fiber leads to 16 tensile test series as summarized in Table 4. For example, the tensile specimen containing 1.0% T-fiber and 0.5% SS-fiber is designated as T10SS05. Three to five specimens per series were prepared for all test series.

4.2. Specimen preparation

A food type laboratory mixer of sixty liter capacity was used to prepare the cement mixture. Cement, silica fume, glass powder and sand were first dry-mixed for about 10 min. Sand and silica fume were first added, and then other ingredients were added to the mixture during dry mixing. Water pre-mixed with polycaboxylate superplasticizer was then added gradually and mixed for another 5–10 min. When the mortar shows enough flow ability for workability and viscosity for uniform fiber distribution, the micro-fibers were dispersed carefully by hand into the mortar mixture, and then the macro-fibers were added. The cement mixture with fibers was then placed in a mold by using a wide scoop with no vibration due to the high flow ability of the mortar mixed with fibers. During mixing and placing of the fresh mixture, care was taken in determining the amount of superplasticizer to prevent steel fiber segregation and to maintain apparent uniform fiber distribution. Although care was taken during mixing and casting, HB-fibers were likely oriented along the axis of the specimen since the length (62 mm) of the HB-fiber is longer than the width (50 mm) of the specimens. Thus, the results would be slightly affected because the HB-fiber is more likely to be aligned to the longitudinal axis of tensile specimens and the alignment of fibers brings favorable conditions to the test results. The specimens were covered with plastic sheets and stored at room temperature for 48 h prior to demolding. Water curing with high temperature (90 ± 2 °C) for 3 days after demolding was carried out. All specimens were tested in dry conditions for 21 days. Two to three layers of polyurethane were sprayed on all surfaces of the specimens after drying to facilitate crack detection.

4.3. Test set-up and procedure

The geometry of test specimen and set-up are shown in Fig. 3. The section of tensile specimens used is 50 × 100 mm (2 × 4 in.), and the gage length of the specimens is 175 mm (7 in.). No steel wire mesh was reinforced at the ends of the specimens to prevent

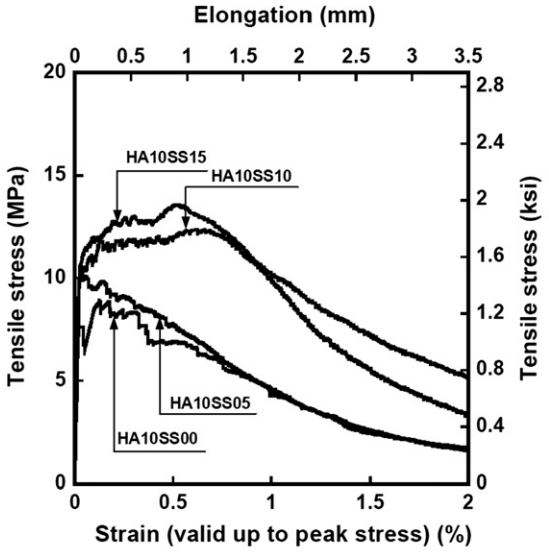

(a) Average tensile stress – strain curves

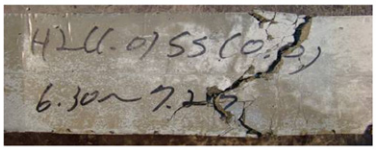

(b) Cracking behavior of HA10SS00

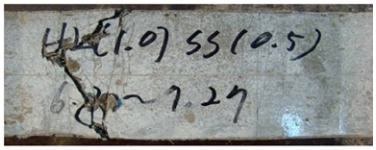

(c) Cracking behavior of HA10SS05

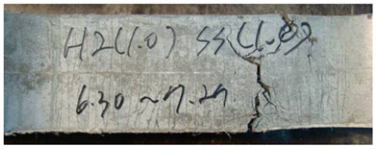

(d) Cracking behavior of HA10SS10

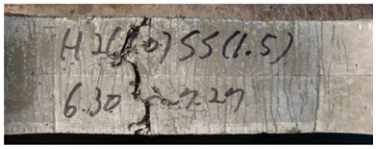

(e) Cracking behavior of HA10SS15

Fig. 5. Tensile test results with high strength steel Hooked A fiber (HA-fiber) as the macro-fiber.

the failure of specimens out of gage length. The alignment of tensile set-up was carefully checked before testing by using a plumb, and the specimens were installed with care to avoid any influence of eccentricity. A universal testing machine (Schmadzu AG-300KNX) running in displacement control was used to conduct the tensile tests. The speed of displacement during testing was 0.4 mm/min (0.016 in./min), and the boundary conditions at both ends of the tensile test set-up are fixed. A special test frame was used to measure the elongation from both sides by using two LVDTs, as shown in Fig. 3 [13]. Elongation of the tensile specimen was obtained from two LVDTs attached to the frame, and the averaged value from the two LVDTs was used in calculating tensile strain until the peak tensile stress. The load signal was measured from a load cell directly attached to the bottom of the cross head.

4.4. Test results and general discussion

The tensile responses of all test series are illustrated by the averaged stress–strain curves in Figs. 4–7 for UHP-HFRCs using LS-, HA-, HB-, and T-fibers as macro-fibers, respectively. Each tensile stress–strain curve in the figures is averaged at least from three specimens except the LS10SS00 series since one specimen of LS10SS00 showed failure within gage length. However, in estimating the averaged σ_{cc} and σ_{pc} of LS10SS00, the results of the five specimens were considered because all the specimens showed strain softening behavior. It should be furthermore noted that the softening part of the average curves in both T10SS00 and T10SS05 series is obtained from one or two specimens while the hardening part is averaged from three specimens since one or two specimens of those series showed the major crack localization, right after peak stress, near the boundary of gage length. Detailed information about the tensile quantities including σ_{cc}, σ_{pc}, ε_{pc}, and number of cracks is summarized in Table 5.

The method of detecting the first cracking strength is illustrated in Fig. 8. If the tensile stress–strain curve shows a clear load drop right after first cracking, as shown in Fig. 8a, the first peak stress in tensile stress–strain curve is selected as first cracking strength. However, if there is no clear first peak point, as shown in Fig. 8b, two lines are drawn from both the linear elastic and hardening parts, and the intersection point between the two lines is selected as first cracking point in this research. This minimizes the subjectivity in determining the first cracking and best represents the first cracking strength.

The number of cracks for each series was obtained by averaging the number of cracks from both sides of specimens, and the number of cracks was counted visually by two investigators to reduce the subjectivity in counting the number of cracks. In counting the number of cracks, it was observed that most micro-cracks went through four surfaces of the specimens.

4.5. Tensile stress–strain responses of UHP-HFRCs

First of all, the overall shape of tensile stress–strain curves of UHP-HFRCs is primarily dependent upon the type of macro-fiber, rather than micro-fiber, as shown in Figs. 4–7. This result confirms once more that there are different roles between macro- and micro-fibers in hybrid systems, as mentioned before by Rossi [21]

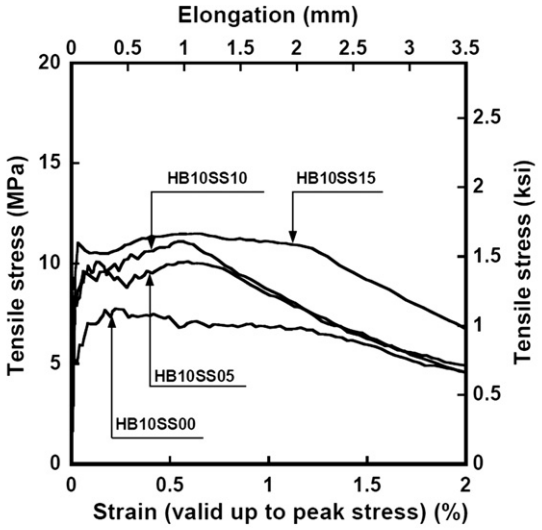

(a) Average tensile stress – strain curves

(b) Cracking behavior of HB10SS00

(c) Cracking behavior of HB10SS05

(d) Cracking behavior of HB10SS10

(e) Cracking behavior of HB10SS15

Fig. 6. Tensile test results with high strength steel Hooked B fiber (HB-fiber) as the macro-fiber.

in the development of high performance multimodal fiber reinforced cement composites.

As shown in Fig. 9, the tensile stress–strain curves of UHP-HFRCs with 1.0% macro-fibers and 1.5% micro-fibers are much different according to the types of macro-fiber, although those series contain higher volume contents of the micro-fibers than the macro-fibers. UHP-HFRC with T-fiber shows the best performance in overall tensile behavior, whereas UHP-HFRC with LS-fiber produces the relatively worst performance among the test series.

It is also noticeable that all UHP-HFRCs tested in this experimental program, with 1.0% macro-fibers and micro-fibers of more than 0.5%, showed strain hardening behavior regardless of the type

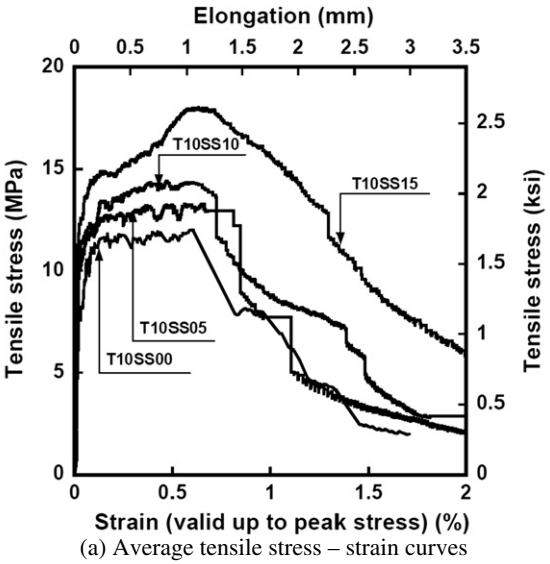

(a) Average tensile stress – strain curves

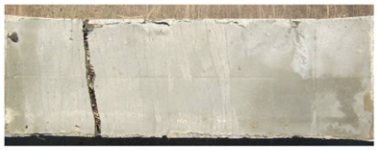

(b) Cracking behavior of T10SS00

(c) Cracking behavior of T10SS05

(d) Cracking behavior of T10SS10

(e) Cracking behavior of T10SS15

Fig. 7. Tensile test results with high strength twisted steel fiber (T-fiber) as the macro-fiber.

Table 5
Average parameter values in tensile behavior of hybrid UHP-FRC.

Notation	First cracking	Post cracking		Number of cracks	Average crack spacing	Number of specimens investigated
	Stress (MPa) Average (standard deviation)	Strain (%) Average (standard deviation)	Stress (MPa) Average (standard deviation)	(ea) Average (standard deviation)	(mm) Average (standard deviation)	
LS10SS00	10.090 (1.314)	0.088 (NA)	8.838 (1.952)	2.00 (NA)	87.50 (NA)	5 for σ_{cc}, σ_{pc}; 1 for others
LS10SS05	9.137 (0.906)	0.322 (0.054)	11.419 (0.484)	4.67 (0.94)	38.89 (10.88)	3 for all
LS10SS10	9.616 (1.265)	0.468 (0.093)	13.305 (0.768)	15.33 (4.03)	12.13 (2.72)	3 for all
LS10SS15	9.880 (0.760)	0.365 (0.055)	13.217 (0.199)	26.67 (3.30)	6.66 (0.80)	3 for all
HA10SS00	7.633 (0.364)	0.182 (0.086)	9.112 (0.458)	2.50 (0.50)	71.92 (14.58)	2 for all
HA10SS05	10.752 (0.285)	0.144b (0.167)	10.895 (0.443)	6.00 (1.41)	30.63 (6.19)	3 for all
HA10SS10	10.056 (0.130)	0.590 (0.111)	12.249 (0.607)	27.00 (2.94)	6.56 (0.68)	3 for all
HA10SS15	10.516 (0.577)	0.562 (0.074)	13.842 (0.542)	34.00 (0.82)	5.15 (0.12)	3 for all
HB10SS00	7.094 (0.857)	0.272 (0.107)	8.054 (0.465)	20.33 (1.70)	8.67 (0.76)	3 for all
HB10SS05	11.350 (0.711)	0.445 (0.210)	10.310 (1.963)	21.50 (10.97)	11.00 (5.87)	4 for all
HB10SS10	9.139 (0.490)	0.594 (0.045)	11.331 (0.635)	31.33 (1.70)	5.60 (0.31)	3 for all
HB10SS15	10.646 (0.369)	0.611 (0.158)	12.014 (1.044)	39.00 (2.16)	4.50 (0.24)	3 for all
T10SS00	7.980 (0.287)	0.303 (0.174)	12.262 (0.341)	31.50 (1.50)	5.57 (0.27)	2 for all
T10SS05	9.707 (1.545)	0.362 (0.199)	13.498 (0.890)	36.67 (1.70)	4.78 (0.22)	3 for all
T10SS10	10.592 (1.575)	0.512 (0.038)	14.772 (0.841)	41.00 (2.94)	4.29 (0.30)	3 for all
T10SS15	10.698 (2.068)	0.636 (0.056)	18.560 (0.162)	46.33 (3.09)	3.80 (0.27)	3 for all

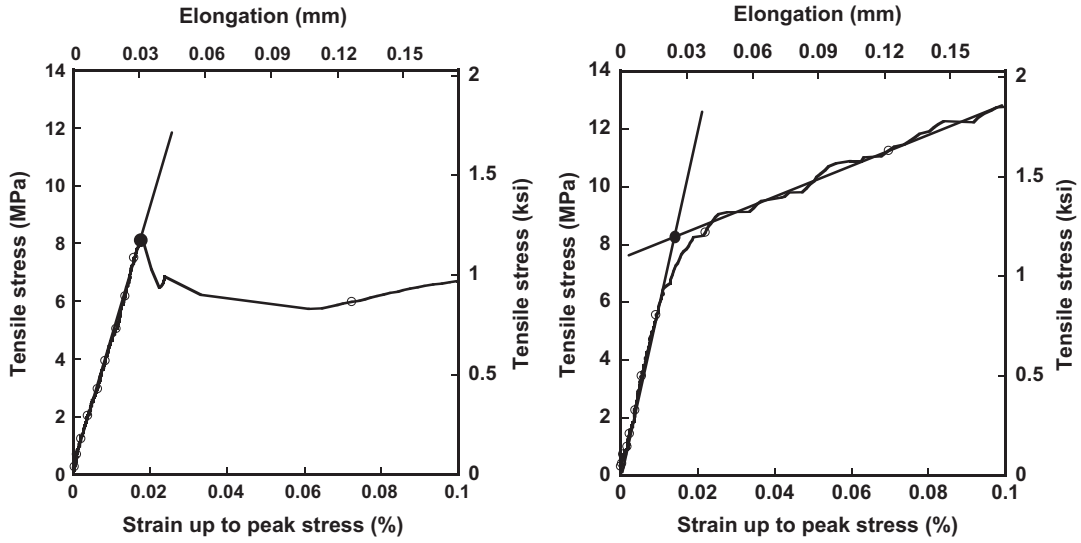

Fig. 8. Detecting the first cracking strength of UHP-HFRC.

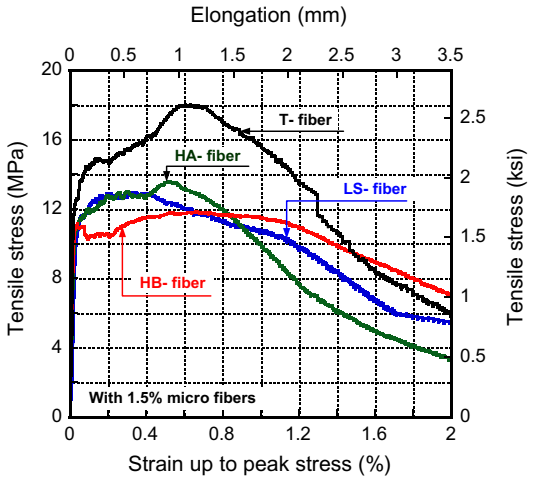

Fig. 9. Comparison of tensile response of UHP-HFRCs with 1.5% micro fibers and 1.0% macro-fibers according to the types of macro-fiber.

of macro-fiber. As the amounts of micro-fiber increase, the tensile quantities including σ_{cc}, σ_{pc}, ε_{pc}, and the number of cracks improved, as shown in Figs. 4–7.

4.6. Multiple cracking behavior of UHP-HFRCs

The cracking behavior of UHP-HFRC is clearly influenced by the type of macro-fiber. Overall, the test series using T-fiber as a macro-fiber (T10SS–) created the highest number of multiple cracks, e.g., 32 for T10SS00, whereas the test series using LS-fiber (LS10SS–) as a macro-fiber produced the lowest number of cracks, e.g., 2 for LS10SS00.

It is clear that the addition of micro-fibers is favorable in creating multiple micro-cracks, as shown in Figs. 4–7 and Table 5. Overall, the number of micro-cracks increases as the volume contents of micro-fiber increase.

4.7. Influence of adding micro-fibers in UHP-HFRCs

To further improve σ_{pc} and ε_{pc} of UHP-HFRCs by adding micro-fibers, it is important to ascertain whether the addition of micro-fibers in UHP-HFRCs is favorable (or not) for strain hardening behavior. If the enhancement of σ_{cc} is higher than that of σ_{pc} by adding micro-fibers in UHP-HFRCs, the addition of micro-fibers in UHP-HFRCs is unfavorable.

Fig. 10 shows the changes of tensile parameters of UHP-HFRC as the amount of micro-fiber increases in hybrid systems. First of all, it is observed that σ_{pc} is more sensitive to the addition of micro-fibers than σ_{cc}, as shown in Fig. 10a and b. As the volume contents of micro-fiber increases from 0.0% to 1.5%, $\Delta\sigma_{cc}$ is between −0.95 MPa and 3.55 MPa, while $\Delta\sigma_{pc}$ varies between 3.96 MPa and 6.30 MPa. Thus, the addition of micro-fibers in UHP-HFRC is favorable for strain hardening behavior.

Furthermore, the number of multiple micro-cracks and ε_{pc} are also enhanced as the volume contents of micro-fiber increase, as shown in Fig. 10c and d. And the averaged crack spacing decreased as the amount of micro-fiber increases, as shown in Fig. 10e. Thus, it is clear that the addition of micro-fibers in UHP-HFRCs favorably affects both strain hardening and multiple micro-cracking behavior.

4.8. Dependence of tensile properties on the type of macro-fiber

The enhancement of tensile properties as the amount of micro-fibers increase is different according to the type of macro-fiber, as shown in Fig. 11. $\Delta\sigma_{cc}$ of UHP-HFRCs with deformed steel macro (HA-, HB- and T-) fibers is between 2.72 MPa and 3.55 MPa with the addition of 1.5% micro-fibers in the hybrid system, while $\Delta\sigma_{cc}$ of UHP-HFRCs with LS-fiber is −0.21 MPa. The different $\Delta\sigma_{cc}$ according to the types of macro-fiber, especially between deformed fibers and LS-fiber, are based on the test results indicating that σ_{cc} of UHP-MFRCs with 1.0% deformed steel (HA-, HB- and T-) fibers is lower than that of UHP-MFRC with 1.0% LS-fiber. During the tensioning process of the specimen, deformed steel fibers generate more damage on the matrix than LS-fiber due to the mechanical interaction between fiber and matrix to activate mechanical bond. Thus, σ_{cc} of UHP-HFRCs with deformed steel fibers is lower than that of UHP-HFRCs with LS-fiber. However, as the amount of micro-fiber increased, the matrix damage from the mechanical interaction was reduced. Thus, UHP-HFRCs with deformed steel fibers as macro-fibers produce higher $\Delta\sigma_{cc}$ than UHP-HFRC with LS-fiber.

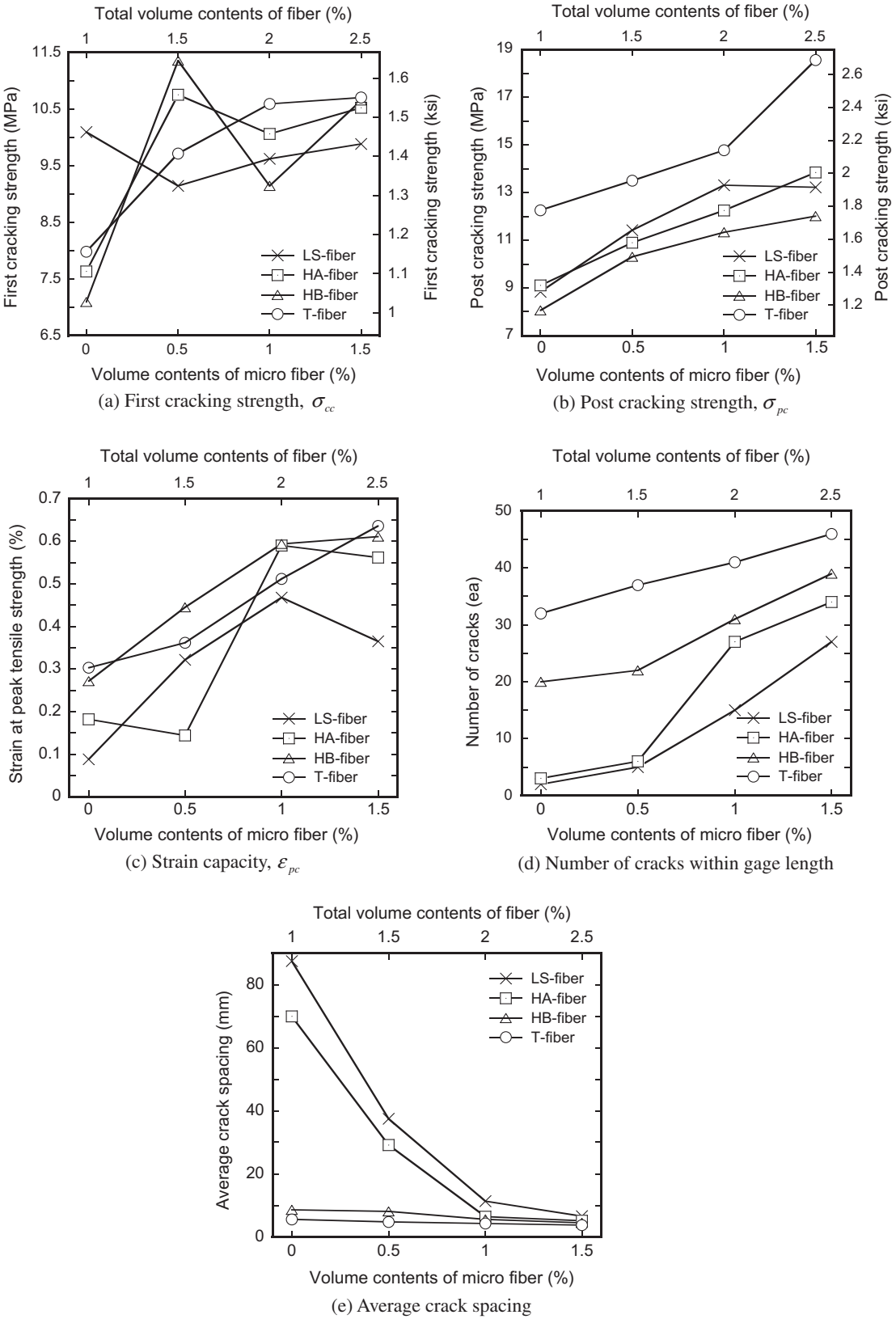

Fig. 10. Influence of micro fiber volume contents on tensile properties of UHP-HFRC.

$\Delta\sigma_{pc}$is also different according to the type of macro-fiber, as shown in Fig. 11b, and varies between 3.96 MPa and 6.30 MPa at the addition of 1.5% micro-fibers. Deformed steel fibers, rather than smooth steel fibers, produce a higher contacting pressure and more damage at the interface between fiber and matrix to activate mechanical bond resistance. Consequently, the different $\Delta\sigma_{pc}$ according to the type of macro-fiber might result from the different degrees of matrix damage.

As shown in Fig. 11c, $\Delta\varepsilon_{pc}$ of UHP-HFRCs are varied between −0.04% and 0.38% according to the types of macro-fiber at the

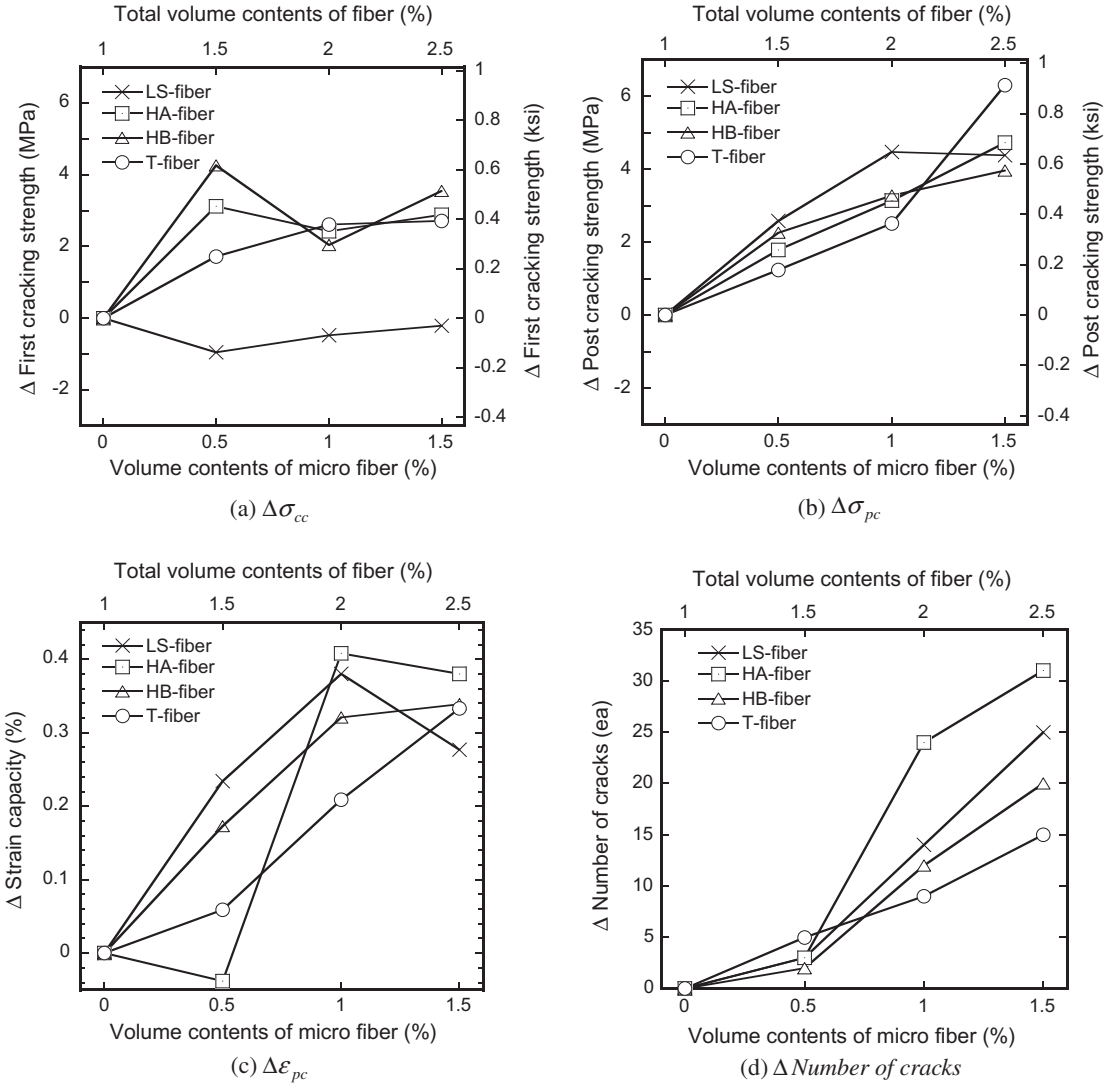

Fig. 11. Dependence of the tensile properties of UHP-HFRC on the type of macro-fiber.

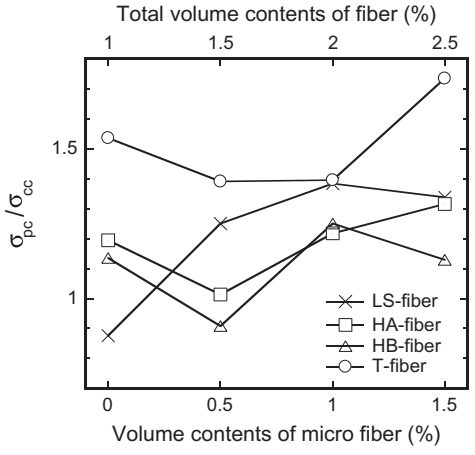

Fig. 12. Influence of adding micro fibers on the ratio between σ_{pc} and σ_{cc}.

addition of 1.5% micro-fiber. However, $\Delta\varepsilon_{pc}$ is not always proportional to the amount of micro-fibers, as shown in Fig. 11c, because $\Delta\varepsilon_{pc}$ depends on the width of micro-cracks as well as the number of micro-cracks. As the amount of micro-fiber increases, the width of cracks decreases while the number of cracks increases. Thus, no clear proportional tendency is observed in $\Delta\varepsilon_{pc}$ as the amount of micro-fiber increases.

The enhancement in the number of cracks as the amount of micro-fiber increased is also different as shown in Fig. 11d according to the type of macro-fiber. By using the tensile prism model suggested by Naaman [18,16] and assuming an equivalent bond strength (τ_{eq}) based on fiber pullout energy [10], the averaged crack spacing can be estimated by using Eq. (2) and is a function of τ_{eq}, which is dependent upon the different pullout mechanism according to the type of macro-fiber, as well as V_f.

$$\text{Average crack spacing}: \Delta L_{av} = \eta \cdot \frac{d_f \cdot (1 - V_f) \cdot \sigma_m}{\alpha_2 \cdot V_f \cdot \tau_{eq}} \tag{2}$$

where η is a factor for the range between minimum and maximum cracking spacing ($1 \leqslant \eta \leqslant 2$), V_f is the volume content of fiber, d_f is the diameter of fiber, σ_m is the tensile strength of matrix, $\alpha_2$is the factor for fiber distribution, and τ_{eq} is the equivalent bond strength.

4.9. Strain hardening ratio σ_{pc}/σ_{cc}

Fig. 12 shows the influence of adding micro-fibers on the strain hardening ratio between σ_{pc} and σ_{cc}. The ratio should be higher

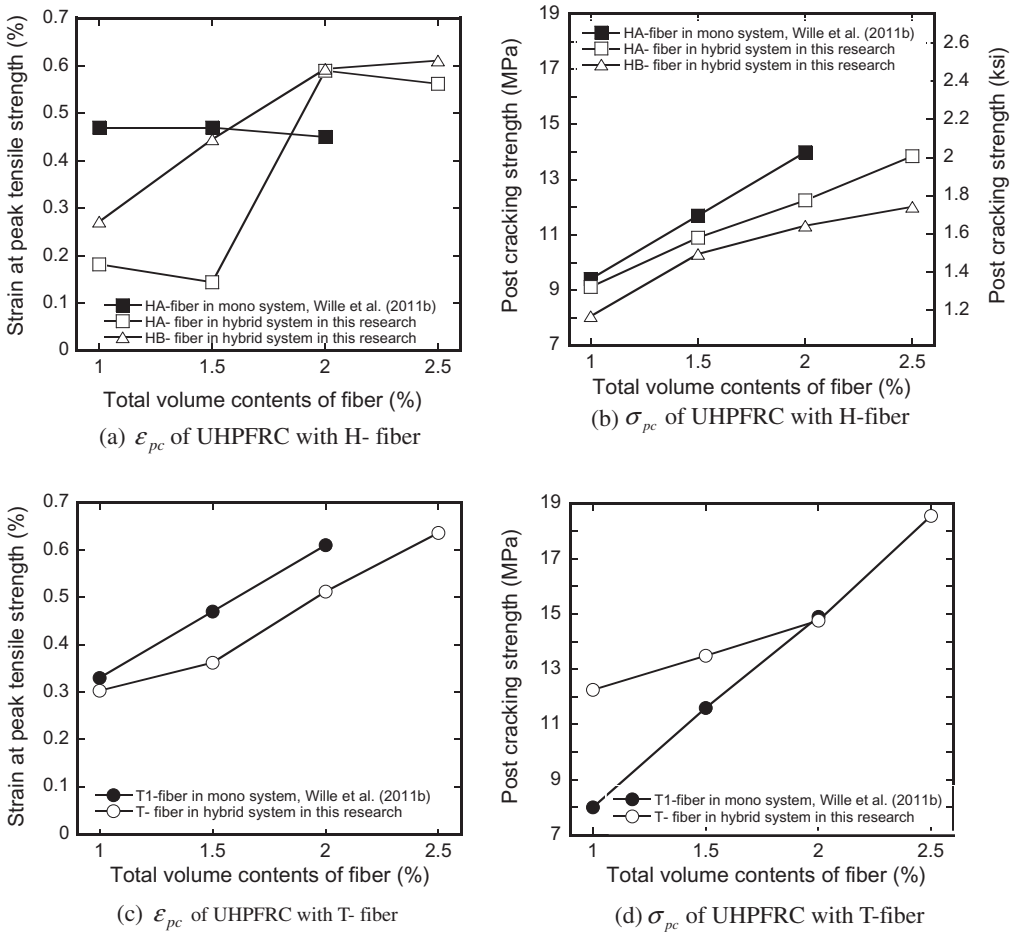

Fig. 13. Comparison of ε_{pc} and σ_{pc} between UHP-MFRC and UHP-HFRC.

than 1.0 to obtain strain hardening behavior, as described in Eq. (1). The strain hardening ratios have been enhanced by adding micro fibers in hybrid systems. However, the ratios are strongly dependent on the type of macro-fiber. T10SS– series showed the highest strain hardening ratio ranging between 1.391 and 1.735 while HB10SS– series produced the lowest values, ranging between 0.908 and 1.240. The higher strain hardening ratio of T-fiber reinforced UHPFRC is based on its unique pullout behavior. Since T-fiber should be untwisted to be pulled out, it utilizes most of the embedded fiber length to generate mechanical resistance, thus the bond resistance of T-fiber is maintained until the slip reaches almost 70–80% of the embedded length of the fiber. The higher slip capacity of T-fiber produces a higher pullout energy, which is related to the higher equivalent bond strength [10].

4.10. Comparison between UHP-HFRC and UHP-MFRC

Fig. 13 compares the tensile performance of UHP-HFRC and UHP-MFRC with HA- and T- fibers. The results of UHP-MFRCs refer to Wille et al. [24], while the data of UHP-HFRCs are obtained from the experimental program performed in this study.

UHP-HFRCs with HA- (or HB-) as macro-fibers also demonstrate a noticeable enhancement of ε_{pc} as the fiber volume content increases, while there is no significant enhancement of ε_{pc} in UHP-MFRC with HA-fibers only. In terms of σ_{pc}, both UHP-MFRC and UHP-HFRC with HA- or HB-fibers showed a linear enhancement of σ_{pc} as the fiber volume content increased, although the hybrid system produced a little lower σ_{pc}. UHP-HFRCs, blending HA- and HB-fibers with micro fibers, produced greater enhancement of ε_{pc} in comparison to UHP-MFRCs.

Whereas UHP-HFRCs with HA-fiber showed higher enhancement in ε_{pc} than UHP-MFRCs as the amounts of (micro) fiber increase, UHPFRCs with T-fiber, both UHP-MFRC and UHP-HFRCs, showed almost linear enhancement in both ε_{pc} and σ_{pc}, as shown in Fig. 13c and 13d.

5. Conclusions

This study investigated the effect of blending macro- and micro-fibers on the tensile stress–strain response of Ultra High Performance Hybrid Fiber Reinforced Concrete (UHP-HFRC). Four types of high strength steel macro-fibers, including long smooth (LS-), two types of hooked (HA- and HB-) and twisted (T-) fiber were investigated. The volume content of the macro-fiber was held at 1.0% while the volume contents of the micro fibers were 0.0%, 0.5%, 1.0% and 1.5%. UHP-HFRCs using 1.0% macro-steel fibers blended with more than 0.5% micro steel fibers produced tensile strain hardening behavior, although they generated different tensile responses according to the type of macro-fiber. The following conclusions can be drawn from this experimental study.

1. The overall shape of the tensile stress–strain curves of UHP-HFRC is primarily dependent upon the type of macro-fiber rather than micro fiber.
2. The addition of micro fibers in hybrid systems produces a favorable effect on both the strain hardening and multiple cracking behavior of UHP-HFRC. As the amount of micro fibers increases,

the tensile properties including ε_{pc}, σ_{pc} and the number of micro cracks were significantly improved, while the increase in σ_{cc} was significant only for the deformed macro-fibers.

3. UHP-HFRC with T-fiber as the macro-fiber produces the best performance in terms of tensile strain hardening behavior: σ_{pc} was 18.6 MPa; ε_{pc} was 0.64%, and the average crack spacing was 3.8 mm.
4. The ranking of performance in terms of post-cracking strength at 1.5% micro fiber volume contents is as follows: T- > HA- > LS- > HB-fibers.
5. The ranking of performance in terms of strain capacity and multiple cracking behavior at 1.5% micro fiber volume contents is as follows: T- > HB- > HA- > LS-fibers.
6. UHP-HFRC with HA-fiber showed greater enhancement in ε_{pc} than UHP-MFRC with the fibers as the amount of fiber increased.

Acknowledgments

This research was sponsored by Super Bridge 200 at the Korea Institute of Construction Technology and financially supported by the Ministry of Knowledge Economy. Further financial support of this research project was granted by the Korea Institute of Energy Technology Evaluation and Planning (2010161010004K). The authors are grateful to those sponsors for financial support. The opinions expressed in this paper are those of the authors and do not necessarily reflect those of the sponsors.

References

[1] Behloul M, Bernier G, Cheyrezy M. Tensile behavior of reactive powder concrete (RPC). In: Proceedings of the 4th international symposium on utilization of HSC/HPC, BHP'96, Paris, vol. 3; 1996. p. 1375–81.
[2] Benson SDP, Karihaloo BL. CARDIFRC–Development and mechanical properties. Part III: Uniaxial tensile response and other mechanical properties. Mag Concrete Res 2005;57(8):433–43.
[3] Boulay C, Rossi P, Tailhan JL. Uniaxial tensile test on a new cement composite having a hardening behavior. In: Proceeding of Sixth RILEM symposium in fiber-reinforced concretes (FRC), BEFIB, Varenna, Italy; 2004.
[4] Chanvillard G, Rigaud S. Complete characterization of tensile properties of DUCTAL® UHP-FRC according to the French recommendations. In: Proceeding of fourth international workshop on high performance fiber reinforced cement composites (HPFRCC4). Ann Arbor, MI, USA; 2003.
[5] Farhat FA, Nicolaides D, Kanellopoulos A, Karihaloo BL. High Performance fiber-reinforced cementitious composite (CARDIFRC) – performance and application to retrofitting. Eng Fract Mech 2007;74(1–2):151–67.
[6] Fehling E, Schmidt M, Geisenhanslueke C, Editor. International symposium on ultra high performance concrete, Kassel, (Schriftenreihe Baustoffe und Massivbau 3); 2004.
[7] Fehling E, Schmidt M, Stuerwald S, editor. Second international symposium on ultra high performance concrete, Kassel, (Schriftenreihe Baustoffe und Massivbau 10); 2008.
[8] Graybeal B, Davis M. Cylinder or cube: strength testing of 80 to 200 Mpa (116 to 29 ksi) Ultra-High-Performance-Fiber-Reinforced Concrete. ACI Mater J 2008;105(6):603–9.
[9] Jungwirth J, Muttoni A. Structural behavior of tension members in Ultra High Performance Concrete. In: International symposium on ultra high performance concrete, Kassel; 2004. p.553–46.
[10] Kim DJ, El-Tawil S, Naaman AE. Correlation between single fiber pullout behavior and tensile response of FRC composites with high strength steel fiber. In: Naaman AE, Reinhardt HW, co-editors. Proceeding of fifth international symposium on high performance fiber reinforced cementitious composites, Mainz, Germany; 2007, pp. 67–76.
[11] Kim DJ, El-Tawil S, Naaman AE. Effect of matrix strength on pullout behavior of high strength deformed steel fibers. In: Parra-Montesinos GJ, Balaguru P, editors. ACI special publication 2010; SP 72, Antoine E. Naaman symposium – four decades of progress in prestressed concrete, fiber reinforced concrete, and thin laminate composites; 2010. p. 135–50.
[12] Kim DJ, Naaman AE, El-Tawil S., High tensile strength strain-hardening FRC composites with less than 2% fiber content. In: Fehling E, Schmidt M, Stűrwald S, co-editors, Proceeding of second international symposium on ultra high performance concrete, Germany, Kassel University, Germany; 2008, p. 169–76.
[13] Sirijaroonchai K, El-Tawil S, Parra-Montesinos G. Behavior of high performance fiber reinforced cement composites under multi-axial compressive loading. Cement Concrete Compos 2010;32(1):62–72.
[14] Maeder U, Lallemant-Gamboa I, Chaignon J, Lombard JP, Ceracem, a new high performance concrete: characterizations and applications. In: Fehling E, Schmidt M, Stűrwald S, co-editors, Proceeding of first international symposium on ultra high performance concrete, Kassel University, Germany; 2004. p. 59–68.
[15] Markovic I. High-Performance Hybrid-Fibre Concrete–Development and Utilization, Ph.D. thesis, Technische Universität Delft; 2006.
[16] Naaman AE. Ferrocement & laminated cementitious composites. Ann Arbor (Michigan, USA): Techno Press 3000; 2000.
[17] Naaman AE, Reinhardt HW. Characterization of high performance fiber reinforced cement composites. In: Naaman AE, Reinhardt HW, co-editors. Proceeding of second international symposium on high performance fiber reinforced cementitious composites; 1996. p. 1–24.
[18] Naaman AE. A Statistical Theory of Strength for Fiber Reinforced Concrete, Ph.D. thesis, Massachusetts Institute of Technology; 1972. p. 196.
[19] Park JJ, Kang ST, Koh KT, Kim SW. Influence of the ingredients on the compressive strength of UHPC as a fundamental study to optimize the mixing proportion. In: Fehling E, Schmidt M, Stűrwald S, co-editors. Proceeding of second international symposium on ultra high performance concrete, Germany, Kassel University, Germany; 2008. p. 105–12.
[20] Rossi P, Antonio A, Parant E, Fakhri P. Bending and compressive behaviors of a new cement composite. Cement Concrete Res 2005;35(1):27–33.
[21] Rossi P. High performance multimodal fiber reinforced cement composite (HPMFRCC): the LCPC experience. ACI Mater J 1997;94(6):478–83.
[22] Ryu GS, Kang ST, Park JJ, Koh GT. Evaluation of flexural performance in UHPC (Ultra High Performance Concrete) according to placement methods. Key Eng Mater 2010:417–8. p. 581–4.
[23] Wille K, Naaman AE, Parra-Montesinos GJ. Ultra-high performance concrete with compressive strength exceeding 150 MPa (22 ksi): a simpler way. ACI Mater J 2011;108(6):46–54.
[24] Wille K, Kim DJ, Naaman AE. Strain hardening UHP-FRC with low fiber contents. Mater Struct 2011;44:583–98.
[25] Wuest J, Denarie E, Bruehwiler E. Model for predicting the UHP-FRC tensile hardening response. In: Fehling E, Schmidt M, Stűrwald S, co-editor. Proceeding of second international symposium on ultra high performance concrete, Germany. Kassel University, Germany; 2008. p. 153–60..